

## Modulation of optical spatial coherence by surface plasmon polaritons

SHAWN DIVITT,<sup>1</sup> MARTIN FRIMMER,<sup>1</sup> TACO D. VISSER,<sup>2,3</sup> AND LUKAS NOVOTNY<sup>1,\*</sup>

<sup>1</sup>Photonics Laboratory, ETH Zürich, 8093 Zürich, Switzerland

<sup>2</sup>Faculty of Electrical Engineering, Mathematics and Computer Science, Delft University of Technology, Delft, The Netherlands

<sup>3</sup>Department of Physics and Astronomy, Vrije Universiteit, Amsterdam, The Netherlands

\*Corresponding author: lnovotny@ethz.ch

Received 28 April 2016; revised 3 June 2016; accepted 4 June 2016; posted 6 June 2016 (Doc. ID 262276); published 29 June 2016

**The interference pattern observed in Young's double-slit experiment is intimately related to the statistical correlations of the waves emitted by the slits. As the waves in the slits become more correlated, the visibility of the interference pattern increases. Here, we experimentally modulate the statistical correlations between the optical fields emitted by a pair of slits in a metal film. The interaction between the slits is mediated by surface plasmon polaritons and can be tuned by the slit separation, which allows us to either increase or decrease the spatial coherence of the emerging fields relative to that of the incoming fields.** © 2016 Optical Society of America

**OCIS codes:** (240.6680) Surface plasmons; (030.0030) Coherence and statistical optics.

<http://dx.doi.org/10.1364/OL.41.003094>

The observation of interference fringes in Thomas Young's double-slit experiment stands as a pivotal moment in wave optics [1]. The spatial modulation of the light intensity on Young's screen can be explained by applying the superposition principle to optical waves emitted by the slits [2]. In more recent years, double- and multi-slit experiments have been applied in evincing the wave nature of matter as well [3,4]. An important aspect of the double-slit experiment is the visibility of the fringes, which is a measure for the contrast between neighboring bright and dark regions in the interference pattern [5].

As long as the superposition principle applies, the fringe visibility is invariably determined by statistical correlations between the waves emitted by the slits, whether they are electromagnetic, matter, or otherwise. That is, the amplitude and phase of the waves act like correlated random variables and information about their correlation can be found in the visibility of the fringes [6]. In optics, the statistical correlation between the electromagnetic fields at two points in space, as a function of frequency, is known as the spectral degree of spatial coherence [7], called hereafter simply the degree of coherence.

Since full control over optical fields includes control over their statistical correlations, several methods for controlling optical spatial coherence have been developed, including spinning

phase diffusers [8], spatial light modulators (SLMs) [9], and digital micromirror devices (DMDs) [10]. Each of these methods generates the equivalent of many phase and amplitude masks that, under ensemble averaging, impart the desired spatial coherence on the outgoing light. However, these masks require a characteristic generation time that is limited by the switching speed of the active device.

It was recently suggested that surface modes of electromagnetic fields at metal-dielectric interfaces, known as surface plasmon polaritons (SPPs), can be used to control the spatial coherence between optical fields [11]. In this case, an ensemble of device realizations is unnecessary to impart the desired degree of coherence. This concept has since attracted significant theoretical attention [12–16]. Experimentally, interference phenomena have been observed in systems that use SPPs to couple two or more emitters [17–22], which indicates that plasmonic control over spatial field correlations, as a function of frequency, is indeed possible. However, an explicit and quantitative demonstration of SPP-controlled modulation of the degree of coherence has remained elusive to date.

In this Letter, we harness the interaction of light and matter to control the degree of coherence between two optical waves of the same frequency. Explicitly, we use SPPs to modulate the degree of coherence between the fields in the two slits of a double-slit experiment [23]. The plasmonic method presented here stands apart from other techniques because the field randomization is passive rather than relying on an ensemble of active device realizations. Accordingly, coherence control based on SPP coupling relies on engineering the generation and propagation of electromagnetic surface waves rather than on the generation of an ensemble of amplitude and phase masks necessary for previous methods.

A sketch of our experiment is given in Fig. 1(a). Light from a spatially extended thermal light source is spectrally bandpass filtered at  $633 \pm 5$  nm wavelength and linearly polarized before it illuminates the double-slit sample, which is mounted in front of a CCD detector that records the generated interference pattern. The sample is a 200 nm thick gold film deposited on glass. Two slits with a width of 400 nm have been created in the metal film, as drawn in Fig. 3(a), using electron beam lithography and argon ion milling. The light impinges onto

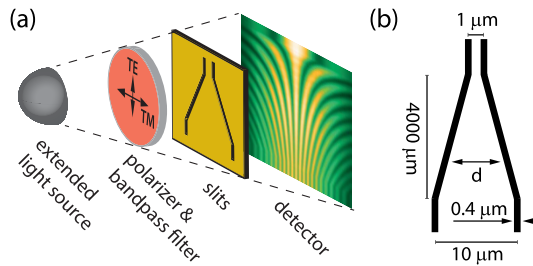


**Fig. 1.** (a) Illustration of the experiment. Filtered and polarized light from an extended thermal source passes through a pair of non-parallel slits in a gold film, creating an interference pattern on a detector (shown in false color). Rotation of the polarizer provides control over the coupling between the incident light and SPPs propagating on the metal film. Existence of these SPPs influences the correlations between the fields in the two slits, which is reflected in the visibility of the interference fringes on the detector. (b) A schematic (not drawn to scale) of the double-slit aperture.

the glass side of the sample. The slits have a length of 4 mm and their separation varies from 1 to 10  $\mu\text{m}$ , as sketched in Fig. 1(b). The parallel parts of the slits serve for reference. With the slit length largely exceeding the slit separation, each horizontal line in the interference pattern encodes the statistical correlations of the fields in the two slits at a specific slit separation  $d$ .

We record two interference patterns using the same double-slit sample. The first one, shown in Fig. 2(a) in false color, is acquired under TE-polarized illumination (electric field vector parallel to the slits). In this case, the incoming field cannot couple to surface modes of the metal-dielectric interface and the slits in the gold film act like a simple binary mask [24]. As expected, we observe the typical interference fringes, where the distance between intensity minima along the horizontal dimension is, to first order, inversely proportional to the slit separation  $d$  and gives each fringe its hyperbolic shape [25]. The second measurement, shown in Fig. 2(b), is taken under TM-polarized illumination (electric field vector perpendicular to the slits). Under these conditions, SPPs are excited at the edges of the slits and propagate across the surface of the gold film [21]. We observe the expected interference fringes as under TE illumination. Strikingly, however, the fringe visibility is modulated with changing slit separation  $d$  under TM-polarized illumina-

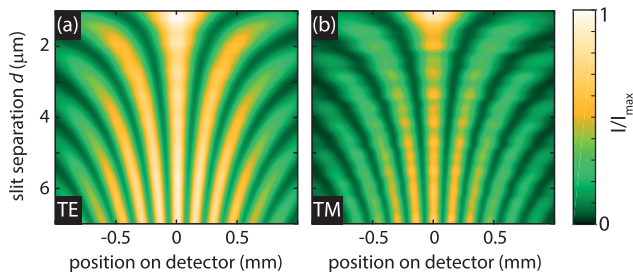


**Fig. 2.** False color images of the interference patterns generated on the detector behind the slits under illumination with (a) TE and (b) TM polarization. The images represent the raw normalized detector intensity ( $I/I_{\text{max}}$ ) used in measuring the degree of coherence vs. the slit separation  $d$ .

tion, in stark contrast to TE-polarized illumination, where the fringe visibility is smooth.

As a quantitative measure for the fringe visibility, we extract the degree of coherence between the fields in the two slits from each horizontal line of each interference pattern at the corresponding slit separation  $d$ , following the method of [25]. A large number of measurements are averaged such that the random error associated with each data point is approximately the size of the plotted symbol. In Fig. 3(b), we plot as blue dots the degree of coherence as a function of slit separation in the range  $3 \mu\text{m} < d < 7 \mu\text{m}$  for TE illumination, as extracted from Fig. 2(a). Since the sample in this case acts like a simple binary mask, the measurement for TE illumination is a characterization of the degree of coherence between the fields in the slits as produced by the bare source. The degree of coherence falls off nearly linearly in  $d$  within the given range under the particular source used. In contrast, the degree of coherence under TM polarization, plotted in Fig. 3(b) as the red crosses, shows a clear modulation on top of the linear fall-off of the TE case. Here, the interaction between the incident TM-polarized radiation and the sample modulates the degree of coherence between the fields in the slits as a function of the slit separation. Notably, this light-matter interaction can both boost the

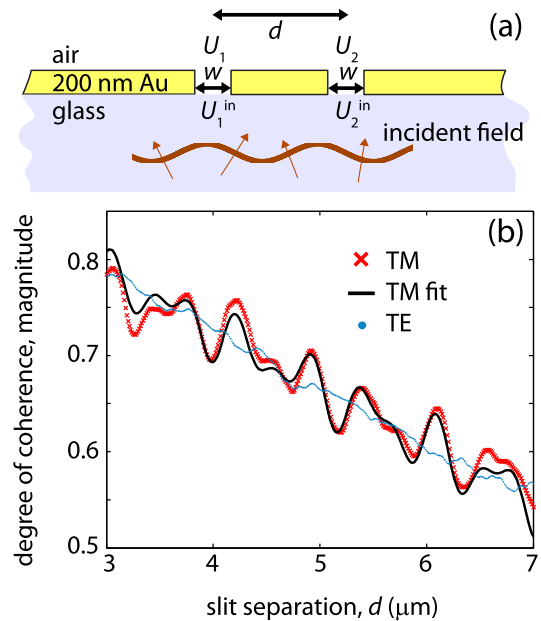


**Fig. 3.** (a) A cross-sectional diagram of the double-slit aperture. Two slits with a width  $w = 400 \text{ nm}$  and a varying separation  $d$  are milled in a 200 nm thick gold film on glass. (b) Measured degree of coherence of light emitted by the double-slit aperture, shown in (a), under incident light of TE (blue dots) and TM polarization (red crosses), as defined in Fig. 1(a). The modulation under TM polarization is the result of coupling via SPPs propagating on both the upper and lower surfaces of the gold layer. Equation (4) was used in generating the fit (black solid line) with the free parameters  $\beta_r = .023$  and  $\beta_b = .026$ . The values for  $k_r = 1.03 \times 10^7 + i3.3 \times 10^4 \text{ m}^{-1}$  and  $k_b = 1.65 \times 10^7 + i1.3 \times 10^5 \text{ m}^{-1}$  are set by material parameters, and a linear fit to the plotted TE curve was used for  $\mu_{12}^{\text{in}}$ . A systematic error due to physical imperfections in the slit widths leads to small but consistent deviations from a smooth curve, readily seen in the TE case, as measured under the method of [25], which assumes identical and perfect slits.

degree of coherence beyond and suppress it below that of the incoming field.

The excitation of SPPs traveling on the metal surface and mediating the coupling between the slits indeed explains the observed modulation of the degree of coherence under TM polarization. A simple model taking into account surface waves fully describes our measurements. Letting  $U_1(\omega)$  and  $U_2(\omega)$  be complex scalar fields at some positions 1 and 2, respectively, with angular frequency  $\omega$ , the degree of coherence between the fields is defined by [5]

$$\mu_{12}(\omega) := W_{12}(\omega) / \sqrt{W_{11}(\omega)W_{22}(\omega)}, \quad (1)$$

where  $W_{nm}(\omega) := \langle U_n^*(\omega)U_m(\omega) \rangle$  is the cross-spectral density (or covariance) function,  $*$  indicates a complex conjugate, and the angle brackets indicate an ensemble average over quasi-monochromatic field realizations.

We now apply Eq. (1) to the SPP-coupled double-slit case to describe the degree of coherence between the fields that *exit* the slits under knowledge of the degree of coherence of the fields that *enter* the slits. We let  $U_1^{\text{in}}(\omega)$  and  $U_2^{\text{in}}(\omega)$  be the fields incident on slits 1 and 2, respectively, as sketched in Fig. 3(a), and  $\mu_{12}^{\text{in}}(\omega)$  be the degree of coherence between them. Following the model of Gan *et al.* [11], we assume that the incident field at each slit can be separated into two parts. The first part is directly transmitted, while the second is converted into SPPs that travel to the other slit and scatter back into freely propagating radiation. Further allowing for different materials at the top and bottom gold interfaces, we express the field  $U_j$  ( $j = 1, 2$ ), leaving slit  $j$  as

$$U_1 = \alpha U_1^{\text{in}} + \alpha\beta_t U_2^{\text{in}} e^{ik_t d} + \alpha\beta_b U_2^{\text{in}} e^{ik_b d}, \quad (2)$$

and

$$U_2 = \alpha U_2^{\text{in}} + \alpha\beta_t U_1^{\text{in}} e^{ik_t d} + \alpha\beta_b U_1^{\text{in}} e^{ik_b d}, \quad (3)$$

where  $\alpha$  is the fraction of the incident field that couples into the slits,  $\beta_t$  and  $\beta_b$  are the fractions of the coupled field that are converted to SPPs on the gold–air and the gold–glass interfaces, respectively,  $k_t$  and  $k_b$  are the wave numbers associated with the surface plasmons at these interfaces, and  $d$  is the slit separation. All the parameters  $\alpha$ ,  $\beta_t$ ,  $\beta_b$ ,  $k_t$ , and  $k_b$  are complex valued and depend on  $\omega$ , in general.

Assuming the incoming power spectral densities at each slit are identical, that is  $W_{11}^{\text{in}}(\omega) = W_{22}^{\text{in}}(\omega)$ , we can insert Eqs. (2) and (3) into Eq. (1). Dropping the dependence on  $\omega$ , we find

$$\mu_{12} = \frac{\mu_{12}^{\text{in}} + 2 \operatorname{Re}(A) + \mu_{12}^{\text{in}*} B}{\sqrt{(1 + 2 \operatorname{Re}[\mu_{12}^{\text{in}} A] + B)(1 + 2 \operatorname{Re}[\mu_{12}^{\text{in}*} A] + B)}}, \quad (4)$$

where  $A := \beta_t e^{idk_t} + \beta_b e^{idk_b}$ ,  $B := |\beta_t|^2 e^{id(k_t - k_t^*)} + |\beta_b|^2 e^{id(k_b - k_b^*)} + 2 \operatorname{Re}(\beta_t \beta_b e^{id(k_b - k_t^*)})$ ,  $\operatorname{Re}$  indicates the real part, and we have used the fact that  $\mu_{21}^{\text{in}}(\omega) = \mu_{12}^{\text{in}*}(\omega)$ . We note that in the absence of SPPs, where  $\beta_t = \beta_b = 0$ , Eq. (4) predicts the entering and exiting degrees of coherence to be identical. Accordingly, the measurement of the degree of coherence under TE illumination is a measurement of  $\mu_{12}^{\text{in}}$ , since no SPPs are excited in that case. With Eq. (4), the degree of coherence between the fields  $U_1$  and  $U_2$  can be predicted given the material parameters, which set the propagation constants  $k_t$  and  $k_b$ , and the degree of coherence between the incident fields,  $\mu_{12}^{\text{in}}$ .

The fit to the TM data, shown as the solid line in Fig. 3(b), was created using Eq. (4). The coupling strengths  $\beta_t$  and  $\beta_b$  were the only fit parameters. While  $\beta_t$  and  $\beta_b$  vary somewhat

for different slit separations due to physical imperfections in the slits themselves, constant values provide a consistent and meaningful approximation. A linear fit of the measured TE curve was inserted for  $\mu_{12}^{\text{in}}$ , and  $k_t$  and  $k_b$  were determined by the material parameters for air (refractive index 1), gold (relative permittivity  $\epsilon = -13 + 1i$ ) [26], glass (refractive index 1.51), and the center free-space wavelength  $\lambda = 633$  nm of the incident light [24]. The fit and the measured curve correspond well, indicating that Eq. (4) successfully describes the degree of coherence between the fields exiting the slits.

To further corroborate that the observed modulation of the degree of coherence indeed relies on the generation of SPPs mediating between the fields in the two slits, we evaporated an optically thin layer of 5 nm of titanium (Ti) onto the gold film. The resulting structure is sketched in Fig. 4(a). We again measure the degree of coherence of the fields in the slits for both TE polarization [blue dots in Fig. 4(b)] and TM polarization (red crosses). For TE polarization, the degree of coherence falls off linearly with slit separation  $d$ , just as for the sample without the titanium layer. For TM polarization, the degree of coherence has a simple sinusoidal modulation in  $d$  sitting atop the linearly sloped incoming coherence function. The modulation of the degree of coherence as a function of slit separation  $d$  for TM illumination is markedly different in the sample after addition of the titanium layer [Fig. 4(b)] as compared to that before adding the titanium layer [Fig 3(b)].

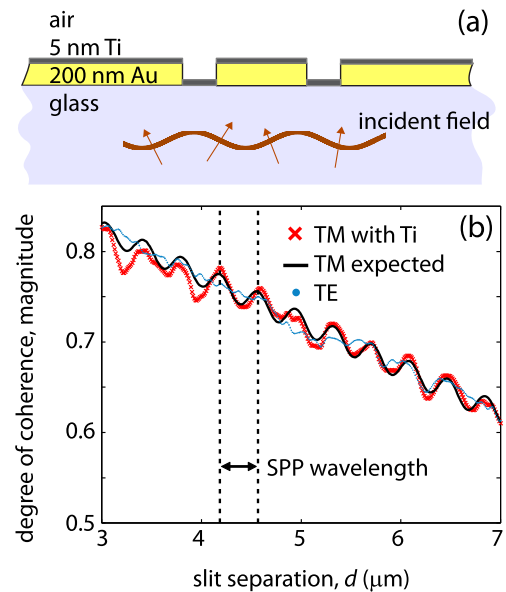


**Fig. 4.** (a) A cross-sectional diagram of the double-slit aperture after being covered with an optically thin (5 nm) layer of titanium. The titanium layer serves to damp SPPs on the top gold surface. (b) The measured degree of coherence of light emitted by the double-slit aperture shown in (a), under incident light of TE (blue dots) and TM polarization (red crosses). Here, the modulation under TM polarization is the result of coupling via SPPs propagating on only the lower surface of the gold layer. Equation (4) was used to calculate the expected curve (solid black line) with  $\beta_t$  set to zero to account for the absence of SPPs on the top gold surface,  $\beta_b$  as extracted from the fit in Fig. 3(b),  $k_b$  set by the material parameters, and inserting a linear fit of the plotted TE curve for  $\mu_{12}^{\text{in}}$ . The systematic error mentioned in Fig. 3 also affects these measurements.

In the absence of the titanium layer, SPPs propagate on both surfaces of the gold layer with different propagation constants, leading to the beat pattern observed in Fig. 3(b). Addition of the titanium layer causes the SPPs propagating on the top interface to be highly damped such that plasmonic coupling occurs only on the gold–glass interface. Since only one SPP wavelength is present, the degree of coherence has a simple sinusoidal modulation in  $d$  under TM polarization. Ignoring damping, Eq. (4) predicts this modulation to have a wavelength equal to the SPP wavelength of  $2\pi/\text{Re}(k_b) = 381$  nm. As shown in Fig. 4(b), the period of modulation is indeed the SPP wavelength, as indicated by the two vertical dashed lines. We stress that the solid line in Fig. 4(b) is not a fit but a calculation according to Eq. (4) with all parameters deduced from independent measurements: the value for  $\mu_{12}^{\text{in}}$  was extracted from a linear fit to the measured curve under TE illumination, the value for  $k_b$  is set by material parameters (and identical to that used in the case without titanium layer),  $\beta_b$  is the fit parameter obtained from the sample without titanium layer, and  $\beta_t$  is set to zero, accounting for the absence of SPPs propagating at the top surface of the gold film. We note that although the modulation depth appears to be constant in both Figs. 3(b) and 4(b), the finite propagation length of the SPPs eventually causes the modulation depth to decrease with increasing  $d$ . The expected and measured TM curves are in excellent agreement, indicating that our simple model successfully accounts for all significant physical mechanisms at play.

Our experimental results clearly demonstrate that surface plasmon polaritons modulate the statistical correlation, also known as the spectral degree of spatial coherence, between the light fields emitted by a double-slit aperture [23]. Our method allows for a controllable increase in the degree of coherence beyond that of the incoming light, and for a reduction in the degree of coherence below that of the incoming light, by changing the separation between the slits. By choosing the metal, illumination wavelength, and slit width, the modulation depth of the degree of coherence between the fields in the two slits can be engineered [27]. Spatial coherence modulation is of considerable interest for applications in optical free-space communications, where partially spatially coherent beams might be more robust against atmospheric or undersea turbulence than coherent beams [28]. More generally, the spatial coherence of a beam determines how it propagates through space [29], and the ability to modulate the coherence of a beam at high speed can serve as a powerful tool for controlling electromagnetic radiation. Current methods of dynamically controlling spatial coherence rely on devices such as SLMs or DMDs, whose switching speeds forbid any high-speed application. The nanophotonic method described here is fundamentally different, and when combined with dynamic SPP control methods [30] will enable integrated spatial coherence switching at extremely high rates.

**Funding.** Swiss National Science Foundation (SNSF) (200021\_149433); Air Force Office of Scientific Research (AFOSR) (FA9550-16-1-0119).

**Acknowledgment.** The authors acknowledge Nick Vamivakas, Miguel Alonso, and Dieter Pohl for fruitful discussions.

## REFERENCES

1. T. Young, *A Course of Lectures on Natural Philosophy and the Mechanical Arts* (J. Johnson, 1807), Vol. 1, pp. 464–465.
2. M. Born and E. Wolf, *Principles of Optics*, 7th ed. (Cambridge University, 1999).
3. C. Jönsson, *Z. Phys.* **161**, 454 (1961).
4. M. Arndt, O. Nairz, J. Vos-Andreae, C. Keller, G. van der Zouw, and A. Zeilinger, *Nature* **401**, 680 (1999).
5. E. Wolf, *Introduction to the Theory of Coherence and Polarization of Light* (Cambridge University, 2007).
6. J. W. Goodman, *Statistical Optics* (Wiley, 2015).
7. E. Collett and E. Wolf, *Opt. Lett.* **2**, 27 (1978).
8. P. D. Santis, F. Gori, G. Guattari, and C. Palma, *Opt. Commun.* **29**, 256 (1979).
9. M. W. Hyde, S. Basu, D. G. Voelz, and X. Xiao, *J. Appl. Phys.* **118**, 093102 (2015).
10. B. Rodenburg, M. Mirhosseini, O. S. M. na Loaiza, and R. W. Boyd, *J. Opt. Soc. Am. B* **31**, A51 (2014).
11. C. H. Gan, G. Gbur, and T. D. Visser, *Phys. Rev. Lett.* **98**, 043908 (2007).
12. C. H. Gan and G. Gbur, *Plasmonics* **3**, 111 (2008).
13. C. H. Gan, Y. Gu, T. D. Visser, and G. Gbur, *Plasmonics* **7**, 313 (2012).
14. T.-T. Bian, B.-Y. Gu, and Y. Zhang, *Opt. Commun.* **283**, 608 (2010).
15. B. Kanseri, H. C. Kandpal, and R. C. Budhani, *Opt. Commun.* **285**, 4811 (2012).
16. T. Saastamoinen and H. Lajunen, *Opt. Lett.* **38**, 5000 (2013).
17. N. Kuzmin, G. W. 't Hooft, E. R. Eliel, G. Gbur, H. F. Schouten, and T. D. Visser, *Opt. Lett.* **32**, 445 (2007).
18. S. Ravets, J. C. Rodier, B. E. Kim, J. P. Hugonin, L. Jacubowicz, and P. Lalanne, *J. Opt. Soc. Am. B* **26**, B28 (2009).
19. S. Aberra Guebrou, C. Symonds, E. Homeyer, J. C. Plenet, Y. N. Gartstein, V. M. Agranovich, and J. Bellessa, *Phys. Rev. Lett.* **108**, 066401 (2012).
20. L. Shi, T. K. Hakala, H. T. Rekola, J.-P. Martikainen, R. J. Moerland, and P. Törmä, *Phys. Rev. Lett.* **112**, 153002 (2014).
21. H. F. Schouten, N. Kuzmin, G. Dubois, T. D. Visser, G. Gbur, P. F. A. Alkemade, H. Blok, G. W. 't Hooft, D. Lenstra, and E. R. Eliel, *Phys. Rev. Lett.* **94**, 053901 (2005).
22. T. Wang, G. Comtet, E. L. Moal, G. Dujardin, A. Drezet, S. Huant, and E. Boer-Duchemin, *Opt. Lett.* **39**, 6679 (2014).
23. R. Carminati and J.-J. Greffet, *Phys. Rev. Lett.* **82**, 1660 (1999).
24. S. A. Maier, *Plasmonics: Fundamentals and Applications* (Springer, 2007).
25. S. Divitt, Z. J. Lapin, and L. Novotny, *Opt. Express* **22**, 8277 (2014).
26. K. M. McPeak, S. V. Jayanti, S. J. P. Kress, S. Meyer, S. Iotti, A. Rossinelli, and D. J. Norris, *ACS Photon.* **2**, 326 (2015).
27. J. Renger, S. Grafström, and L. M. Eng, *Phys. Rev. B* **76**, 045431 (2007).
28. G. Gbur, *J. Opt. Soc. Am. A* **31**, 2038 (2014).
29. L. Mandel and E. Wolf, *Optical Coherence and Quantum Optics* (Cambridge University, 1995).
30. D. Pacifici, H. J. Lezec, and H. A. Atwater, *Nat. Photonics* **1**, 402 (2007).